**Smart Structures and Systems**, *Vol. 16, No. 5 (2015) 919-935*
DOI: http://dx.doi.org/10.12989/sss.2015.16.5.919


# EMD-based output-only identification of mode shapes of linear structures

Soheil Ramezani[a] and Omid Bahar[*]

*Department of Structural Engineering, International Institute of Earthquake Engineering and Seismology, 21 Arghavan, North Dibajee, Farmanieh, Tehran, Iran*

*(Received November 5, 2012, Revised May 18, 2014, Accepted June 2, 2014)*

**Abstract.** The Hilbert-Huang transform (HHT) consists of empirical mode decomposition (EMD) and Hilbert spectral analysis. EMD has been successfully applied for identification of mode shapes of structures based on input-output approaches. This paper aims to extend application of EMD for output-only identification of mode shapes of linear structures. In this regard, a new simple and efficient method based on band-pass filtering and EMD is proposed. Having rather accurate estimates of modal frequencies from measured responses, the proposed method is capable to extract the corresponding mode shapes. In order to evaluate the accuracy and performance of the proposed identification method, two case studies are considered. In the first case, the performance of the method is validated through the analysis of simulated responses obtained from an analytical structural model with known dynamical properties. The low-amplitude responses recorded from the UCLA Factor Building during the 2004 Parkfield earthquake are used in the second case to identify the first three mode shapes of the building in three different directions. The results demonstrate the remarkable ability of the proposed method in correct estimation of mode shapes of the linear structures based on rather accurate modal frequencies.

**Keywords:** output-only modal identification; mode shapes; Hilbert-Huang transform; empirical mode decomposition; intrinsic mode function; UCLA Factor Building

## 1. Introduction

During the last decades, through the development of measuring devices, experimental dynamic analysis has experienced a tremendous growth. Experimental modal analysis as the main part of the experimental dynamic analysis aims to extract structural modal characteristics by both input-output and output-only methods. Output-only methods are less intrusive and expensive compared to input-output methods and consequently are more popular in practice. In output-only analysis (also named as operational modal analysis, ambient modal analysis or natural excitation modal analysis) of civil engineering structures, signal processing techniques including both time and frequency domain techniques are applied (Cunha and Caetano 2006).

As a breakthrough to the traditional signal processing methods, Huang *et al*. (1998) proposed a method for analysis of non-stationary and nonlinear signals, which was called later as the

∗Corresponding author, Assistant Professor, E-mail: omidbahar@iiees.ac.ir
[a] Ph.D. student, E-mail: s.ramezani@iiees.ac.ir


http://www.techno-press.org/?journal=sss&subpage=8 ISSN: 1738-1584 (Print), 1738-1991 (Online)

Hilbert-Huang transform (HHT) method. The HHT method consists of empirical mode decomposition (EMD) and Hilbert spectral analysis. EMD decomposes a signal into a finite intrinsic mode functions (IMFs) and then, the Hilbert transform presents time-frequency-amplitude distribution of IMFs in a spectrum termed as Hilbert spectrum. Applications of HHT have revealed its ability in providing more physically meaningful features than conventional methods for nonlinear and non-stationary signal analysis (Huang *et al.* 1998, Zhang *et al*. 2003, Liu and Xu 2006).

In structural engineering, HHT has been successfully applied for modal identification of structures (Yang and Lei 2000, Yang *et al.* 2003a, Yang *et al*. 2003b, Xu *et al*. 2003, Yang *et al*. 2004, Yan and Miyamoto 2006, Poon and Chang 2007, Bao *et al.* 2009, Liu *et al*. 2011, Wang and Chen 2012). Yang and Lei (2000) and Yang *et al*. (2003a, b) proposed an HHT-based method for modal identification of linear structures in which the modal parameters related to each mode are determined from its free vibration modal response using a band-pass filter and EMD technique. They also applied the HHT method in conjunction with the random decrement technique (RDT) for identification of structures under ambient vibration. Following the same technique, Xu *et al*. (2003) and Yang *et al*. (2004) identified the modal frequencies and damping ratios of two different tall buildings under wind excitations. Poon and Chang (2007) applied EMD for the identification of nonlinear elastic structures under free vibration. In their work, the nonlinear responses estimated through EMD are utilized in a proposed nonlinear normal mode method to extract the properties of nonlinear elastic structures.

Applying the technique proposed by Yang and Lei (2000) and Yang *et al*. (2003a), Yan and Miyamoto (2006) identified the modal frequencies and damping ratios of a benchmark bridge under ambient excitations. Bao *et al*. (2009) proposed a new HHT method for identification of time-varying nonlinear systems with closely-spaced modes. In their method, auto-correlation function of structural response is considered as input, and also a combination of a band-pass filter method and an IMF selection principle are applied to overcome modal perturbation issues. Recently, Liu *et al*. (2011) proposed an output-only system identification method based on EMD, RDT and the Ibrahim Time Domain method. Liu *et al*. (2011) applied their method for modal identification of a three degree-of-freedom (DOF) model and a bridge structure subjected to ambient base excitations. More recently, Wang and Chen (2012) proposed a recursive HHT method for identification of shear multi-story buildings, by which, given floor masses and measured responses, the stiffness and damping in each floor can be monitored. In most of the HHT-based identification techniques such as those briefly described here, the output-only parameter identification is limited to identification of modal frequencies and damping ratios (e.g., Yang and Lei 2000, Yang *et al.* 2003a, Yang *et al*. 2003b, Bao *et al*. 2009, Liu *et al*. 2011) and identification of the mode shapes is not often carried out.

In this paper, as an improvement to the technique applied by Yang et al. (2003a), a new simple and efficient method for output-only identification of mode shapes of linear structures is proposed. In the proposed method, estimated modal responses which are extracted by applying the band-pass filter and EMD technique are directly used to estimate mode shapes of a structure. Hence, there is no need to convert out put responses to free vibration modal responses, which is applied by Yang et al. (2003a). Having rather accurate estimates of the modal frequencies from the measured responses, the proposed method is capable to extract corresponding mode shapes. To demonstrate the accuracy and efficacy of the proposed method, two case studies are considered. The simulated responses obtained from an analytical structural model with known dynamical properties are analyzed in the first case by which the performance of the method in accurate estimation of the mode shapes is validated. In the second case, the first three mode shapes of the UCLA Factor Building in three separate directions using the recorded low-amplitude responses of the building during the 2004 Parkfield earthquake are extracted. In this case, the estimated mode shapes are verified by comparison with those reported in the literature. Before the explanation of the proposed method, the original HHT method is briefly described in the next section.

## 2. Hilbert-Huang transform

HHT consists of two parts; EMD and Hilbert spectral analysis. EMD as the key part decomposes a signal into a finite number of intrinsic modal functions (IMFs) which guarantee a well-behaved Hilbert transform (Huang *et al*. 1998) and then, Hilbert spectral analysis presents time-frequency-amplitude distribution of the signal through the Hilbert transform. By definition, an IMF is any function that satisfies two conditions: (1) in the whole data set, the number of extremes and the number of zero crossings must either equal or differ at most by one; and (2) at any point, the mean value of the envelope defined by the local maxima and the envelope defined by the local minima is zero.

The EMD procedure in its original form suggested by Huang *et al.* (1998) can be summarized in five steps as follows. For a given signal, $s(t)$, with at least one maximum and one minimum, (1) find all the local extreme a, (2) connect all the local maxima by a cubic spline interpolant function as the upper envelope, $e_{max}(t)$, and repeat the procedure for the local minima to achieve the lower envelope, $e_{min}(t)$, (3) compute the average: $l_1(t) = [e_{max}(t) + e_{min}(t)]/2$, (4) let $h_1(t) = s(t) - l_1(t)$, if $h_1(t)$ is not an IMF, repeat steps 1 to 4 on $h_1(t)$ to obtain the first IMF, $c_1(t)$, (5) define residue signal through $d_1(t) = s(t) - c_1(t)$; and repeat steps 1 to 5 on $d_1(t)$ to extract $k$ IMFs. At the end, $s(t)$ is decomposed to $k$-separate IMFs and a residue, $d_k(t)$, which is either a mean trend or a constant. By applying EMD, $s(t)$ can be decomposed as Eq. (1). Among the IMFs, $c_1(t)$ and $c_k(t)$ include the highest and the lowest frequency range, respectively.

$$s(t) = \sum_{i=1}^{k} c_i(t) + d_k(t) \tag{1}$$

For any real-valued function $c(t)$ of $L^P$ class, the Hilbert transform, $y(t)$, is defined by

$$y(t) = \frac{1}{\pi} P \int_{-\infty}^{\infty} \frac{c(\tau)}{t-\tau} d\tau \tag{2}$$

where $P$ indicates the principal value of the singular integral. With the Hilbert transform, the analytic signal, $a(t)$, is defined as

$$a(t) = c(t) + \mathbf{i}\, y(t) = A(t)\, e^{\mathbf{i}\theta(t)} \tag{3}$$

in which

$$A(t) = \sqrt{c^2(t) + y^2(t)} \quad , \quad \theta(t) = \arctan\left(\frac{y(t)}{c(t)}\right) \tag{4}$$

where $A(t)$ and $\theta(t)$ stand for the envelope (instantaneous amplitude) and the phase function, respectively. Instantaneous frequency is defined as the derivative of the phase function

$$\omega(t) = \frac{d\theta(t)}{dt} \tag{5}$$

Having above definitions, $c(t)$ can be written as

$$c(t) = \Re(a(t)) = \Re(A(t)e^{\mathbf{i}\theta(t)}) = A(t)\cos\theta(t) \tag{6}$$

in which $\Re(\cdot)$ indicates the real part of a complex number. Based on the Hilbert spectral analysis, $c(t)$ and its corresponding Hilbert transform, $y(t)$, are defined as $A(t)\cos\theta(t)$ and $A(t)\sin\theta(t)$ respectively. $A(t)$ is a positive-valued function and $\theta(t)$ is a monotonic increasing function. If $c(t)$ represents an IMF, $s(t)$ can be expressed as the following form

$$s(t) = \Re\left\{\sum_{i=1}^{k} A_i(t)e^{\mathbf{i}\int \omega_i(t)dt}\right\} \tag{7}$$

In Eq. (7), $d_k(t)$ is deliberately omitted, because it is either a monotonic function, or a constant. Eq. (7) can be used to represent time-frequency distribution of the amplitude in a spectrum which is termed as Hilbert spectrum, $H(\omega,t)$.

## 3. Proposed method for output-only identification of mode shapes

Generally, structures accept excitations from two sources. The first source excites body of a structure, which affects its free DOFs, and the other excites its supports, which affects supported ones. As a result, the dynamic response of the structure is a function of displacement at both free and supported DOFs. For a linear time-invariant (LTI)$n$-DOF structure, dynamic equation of motion under force and support excitations (Chopra 2001) can be expressed as

$$\begin{bmatrix} \mathbf{M_{ff}} & \mathbf{M_{fs}} \\ \mathbf{M_{fs}^T} & \mathbf{M_{ss}} \end{bmatrix} \begin{Bmatrix} \ddot{\mathbf{X}}_\mathbf{f}^\mathbf{t}(t) \\ \ddot{\mathbf{X}}_\mathbf{s}^\mathbf{t}(t) \end{Bmatrix} + \begin{bmatrix} \mathbf{C_{ff}} & \mathbf{C_{fs}} \\ \mathbf{C_{fs}^T} & \mathbf{C_{ss}} \end{bmatrix} \begin{Bmatrix} \dot{\mathbf{X}}_\mathbf{f}^\mathbf{t}(t) \\ \dot{\mathbf{X}}_\mathbf{s}^\mathbf{t}(t) \end{Bmatrix} + \begin{bmatrix} \mathbf{K_{ff}} & \mathbf{K_{fs}} \\ \mathbf{K_{fs}^T} & \mathbf{K_{ss}} \end{bmatrix} \begin{Bmatrix} \mathbf{X}_\mathbf{f}^\mathbf{t}(t) \\ \mathbf{X}_\mathbf{s}^\mathbf{t}(t) \end{Bmatrix} = \begin{Bmatrix} \mathbf{F_f}(t) \\ \mathbf{F_s}(t) \end{Bmatrix} \tag{8}$$

where in, respectively, $\mathbf{M_{ff}}$, $\mathbf{C_{ff}}$, $\mathbf{K_{ff}}$ are mass, damping, stiffness matrices related to the free DOFs, and $\mathbf{M_{ss}}$, $\mathbf{C_{ss}}$, $\mathbf{K_{ss}}$ are matrices related to the supported DOFs, and $\mathbf{M_{fs}}$, $\mathbf{C_{fs}}$, $\mathbf{K_{fs}}$, are those related to the interaction between free and supported DOFs; also, $\mathbf{X}_\mathbf{f}^\mathbf{t}(t)$ and $\mathbf{F_f}(t)$ are the absolute displacement and force vectors at the free DOFs, $\mathbf{X}_\mathbf{s}^\mathbf{t}(t)$ and $\mathbf{F_s}(t)$ are those at the supported DOFs, respectively. In reality, there is a discrepancy between the measured responses and the theoretical responses in Eq. (8), which is considered here as noise.

The measured response at free DOFs can be expressed as the sum of the theoretical response and the noise

$$\mathbf{Z_f}(t) = \mathbf{X}_\mathbf{f}^\mathbf{t}(t) + \mathbf{N_f}(t) \tag{9}$$

where $\mathbf{Z_f}(t)$ is the real measured response at the free DOFs and $\mathbf{N_f}(t)$ is the noise over $\mathbf{X}_\mathbf{f}^\mathbf{t}(t)$.

In a modal expansion form, $\mathbf{Z_f}(t)$ can be expressed as the linear combinations of the modal vectors

$$\mathbf{Z_f}(t) = \sum_{j=1}^{r} \mathbf{\Phi}_j v_j^t(t) \tag{10}$$

in which $\mathbf{\Phi}_j = [\phi_{1,j}, \phi_{2,j}, \ldots, \phi_{r,j}]^T$, $v_j^t(t)$ and $r$ are, respectively, the $j$th normal modal vector, the $j$th absolute modal coordinate and the number of the free DOFs. The $v_j^t$s in Eq. (10), represent the contribution of $\mathbf{\Phi}_j$s in the absolute measured responses of the structure.

By substituting $\mathbf{X_f^t}(t)$ from Eq. (9) into the first row of Eq. (8), and using orthogonality properties of the mode shapes with respect to $\mathbf{M_{ff}}$ and $\mathbf{K_{ff}}$, and also applying the assumption of the classical damping, $n$-decoupled equations can be obtained as

$$\begin{aligned} &\ddot{v}_j^t(t) + 4\pi\xi_j f_j \dot{v}_j^t(t) + 4\pi^2 f_j^2 v_j^t(t) = \\ &\mathbf{\Phi}_j^T[\mathbf{F_f}(t) - \mathbf{M_{sf}}\ddot{\mathbf{X}}_\mathbf{s}^\mathbf{t}(t) - \mathbf{C_{sf}}\dot{\mathbf{X}}_\mathbf{s}^\mathbf{t}(t) - \mathbf{K_{sf}}\mathbf{X_s^t}(t) + \mathbf{M_{ff}}\ddot{\mathbf{N}}_\mathbf{f}(t) + \mathbf{C_{ff}}\dot{\mathbf{N}}_\mathbf{f}(t) + \mathbf{K_{ff}}\mathbf{N_f}(t)]/m_j \end{aligned} \tag{11}$$

where $f_j$, $\xi_j$, and $m_j$ are respectively the $j$th modal frequency, the $j$th modal damping ratio and the $j$th modal mass of the structure. The noise-dependent terms in Eq. (11) can be considered as additional excitations on the free DOFs. Since the right hand side of Eq. (11) is generally immeasurable, in output-only identification approach, the modal parameters are extracted without knowledge of the input excitations.

Based on the dynamic properties of the LTI systems, the frequency response functions (FRFs) of a multi-DOF structure act as band-pass filters around the modal frequencies. Thus, the band-pass and EMD technique proposed by Yang *et al*. (2003a) can be applied to the measured responses to estimate the modal responses. To apply this technique, the accurate estimates of the modal frequencies are required.

### *3.1 Estimation of the modal frequencies*

In the frequency domain, the peaks in the FRFs of a low-damped multi-DOF system lie around the modal frequencies. Because the input excitations are not taken into consideration in the ambient modal analysis, the FRFs are replaced by the Power Spectral Densities (PSDs) of the output responses. The Welch’s method is one of the methods that can be used for the estimation of the PSDs. By normalizing the individual PSDs and then averaging between all the normalized PSDs, an averaged normalized PSD (ANPSD) is obtained from which the modal frequencies can be identified. In the Peak Picking (PP) method, the frequencies corresponding to the peaks in ANPSD are picked up as the estimates of the modal frequencies of the structure.

In the PP method, it is assumed that: (1) the excitations represent a white noise process, (2) the modal damping is not significantly high and (3) the modal frequencies are not closely-spaced. These assumptions are often valid for most of civil structures under ambient excitations; hence, the PP method can be applied for the accurate estimation of the modal frequencies. Alternatively, any method such as HHT or enhanced HHT (Bahar and Ramezani 2014) that are able to provide the estimates of the modal frequencies may be used instead of the PP method.

### 3.2 Estimation of the modal responses

To estimate the modal responses, the band-pass filtering and EMD technique is applied. In this technique, the output responses are band-passed filtered around the estimated modal frequency and the resulting time histories are processed through EMD, then the corresponding first IMFs are taken as the estimates of the modal responses. By applying this technique around the $j$th estimated modal frequency for all the acceleration responses, an appropriate estimate of the $j$th absolute modal acceleration response of the structure (i.e., $\mathbf{\Phi}_j \ddot{v}_j^t(t)$ ) can be estimated as $\mathbf{I}_j(t) = [I_{1,j}(t), I_{2,j}(t), \ldots, I_{r,j}(t)]^T$ .As a result, the ratio of the modal elements, $\phi_{p,j}/\phi_{q,j}$ $(p, q = 1, 2, \ldots, r)$, may be estimated as $I_{p,j}(t)/I_{q,j}(t)$.

Theoretically, the ratio between the modal elements is constant, but due to phase-shift effects caused by a variety of issues including noise effects, variations in the EMD algorithm (Rilling *et al.* 2003, Wu and Huang 2008) and also variations in type of band-pass filtering, the ratio of $I_{p,j}(t)$ to $I_{q,j}(t)$ is not constant and oscillates around a constant value. Moreover, the phase shift may cause very large outliers due to division by near zero values. Employing the displacement responses which contain much less zero crossings instead of the acceleration responses may reduce the phase-shift effects; however, it is not very efficient in practice.

### 3.3 Estimation of the ratio between modal elements

In the HHT method, an IMF can be considered as a both amplitude and frequency modulated signal in the form of $A(t)\cos\theta(t)$ in which, the variation information of the amplitude and phase function are carried in $A(t)$ and $\cos\theta(t)$, respectively. As a result, the phase variation (including phase shifts) is contained in $\cos\theta(t)$, and $A(t)$ is not considerably influenced by the phase-shift effects. Using this property, the ratio between IMFs can be replaced by the one between the envelopes to bypass the phase-shift effects. The ratio obtained by using the envelopes still oscillates around a constant value due to imperfections in the HHT method, but the amplitude and frequency of the oscillation is strongly reduced. Regarding to the mathematical limitations of the Hilbert transform in accurate determination of the envelope and phase (Huang and Bethesda 2005), in the proposed method, the envelope is considered as the piecewise cubic polynomials which run through the local maxima of an IMF according to (Huang and Bethesda 2005).

The mean trend of $A_{p,j}(t)/A_{q,j}(t)$ can be considered as the good estimate of $|\phi_{p,j}|/|\phi_{q,j}|$ in which, $A_{p,j}(t)$ and $A_{q,j}(t)$ are the envelopes corresponding to $I_{p,j}(t)$ and $I_{q,j}(t)$, respectively. On the other hand, the sign of the ratio of the modal elements can be directly determined from the sign of the mean trend of $I_{p,j}(t)/I_{q,j}(t)$ .It should be noted that unlike $A_{p,j}(t)/A_{q,j}(t)$, $I_{p,j}(t)/I_{q,j}(t)$ is sensitive to the phase-shift effects, therefore, the minimum phase shift in band-pass filtering is necessary for the determination of the sign of the ratio of the modal elements.

To determine the mean trends for both $A_{p,j}(t)/A_{q,j}(t)$ and $I_{p,j}(t)/I_{q,j}(t)$, a robust mean estimator is proposed with the following steps: (1) Let $\lambda$ be a positive and predefined constant value, (2) determine the mean and standard deviation of data as $\mu_1$ and $\sigma_1$, respectively, (3) repeat step 2 for data which fall between $\mu_1 - \lambda\sigma_1$ and $\mu_1 + \lambda\sigma_1$ to obtain $\mu_2$ and $\sigma_2$, (4) iterate on step 2 and 3 until converged values for the mean and standard deviation are obtained as $\mu$ and $\sigma$, respectively. The converged mean obtained by this procedure (i.e., $\mu$) is considered as the mean trend of data. Characteristically, $\mu$ lies where the density of data is highest. In the present work, $\lambda$ is taken equal to 1.0 since the variation of $\lambda$ within the range around 1.0 showed no significant effect on the results of the selected case studies.

Applying the proposed mean estimator, the ratio of the modal elements can be defined as Eq. (12)

$$\phi_{p,j} / \phi_{q,j} = \mu_{A,p,q,j}\, \mathrm{sgn}(\mu_{I,p,q,j}) \qquad p,q = 1,2,...,r \tag{12}$$

In which $\mu_{A,p,q,j}$ and $\mu_{I,p,q,j}$ stand for the mean trends of $A_{p,j}(t)/A_{q,j}(t)$ and $I_{p,j}(t)/I_{q,j}(t)$, respectively and $\mathrm{sgn}(\cdot)$ is the sign function. Once the normalizing DOF/DOFs are determined for the different modes, Eq. (12) can be used for the estimation of the mode shapes. The DOFs which are expected to be very close to the location of the nodes (i.e., zero crossings) in the mode shapes should not be selected as the normalizing DOFs. For such DOFs, the envelopes of the estimated modal responses fluctuate near zero in a characteristic manner. As a result, the negative effects similar to those caused by the phase shift may arise if the DOFs very close to the nodes are selected for the normalization procedure.

Eq. (12) leads to accurate results if two conditions are met; first, the frequency of the *j*th mode (i.e., the center frequency of the band-pass filter) should be correctly estimated and second, with respect to the closeness of the modal frequencies of the structural system, a correct frequency band (i.e., the bandwidth of the band-pass filter) should be applied. For systems with non-closely-spaced modal frequencies (which is in the scope of this paper), only the correct estimates of the modal frequencies need to be applied. In such systems, the modal responses are well-separated in the frequency domain and the variation of the bandwidth applied for the isolation of the modal responses has no significant effect on the results obtained by the proposed method as it is shown by a parametric study in the first example case.

As noted above, in the output-only identification, the FRFs of the structure which give the modal frequencies and mode shapes are unknown because the input excitations are actually unknown. Without having the FRFs, the estimated modal frequencies and mode shapes always need to be examined in order to distinguish between reliable and unreliable mode shapes. In the ANPSD obtained from the output responses, besides the peaks at the modal frequencies, some other peaks which result in distorted mode shapes may appear (due to the violation of the assumptions of the PP method);hence, depending on the type of the structure, different criteria may be applied based on engineering judgment to exclude unreliable mode shapes and their corresponding modal frequencies.

## 4. Case studies

In this section, two case studies are presented to demonstrate the accuracy and efficiency of the proposed method. Numerically simulated responses obtained from an analytical model of a

3-storybuilding with known modal vectors subjected to a Gaussian random base acceleration is analyzed in the first case and the accuracy of the extracted mode shapes are validated by comparison with the theoretical mode shapes. In the second case, the 2004 Parkfield earthquake response data measured from the UCLA Factor Building are processed and the shapes of the first three modes of the building in east-west, north-south and torsional directions are identified; in this case, verification is carried out by comparing the results from the proposed method with those from the existing updated model of the building.

### *4.1 An analytical building model*

An analytical model of a 2D linear 3-story shear building is considered in this case study. The mass and stiffness values of the structure are respectively as follows: $M_1 = M_2 = M_3 = 1000\,kg$, $K_1 = K_2 = 2K_3 = 1000\,kN/m$. With assumption of Rayleigh damping, the same damping ratio of 5% is considered for the first and third modes. The eigenvalue analysis is performed to extract the modal characteristics of the structure as are given in Table 1.The proportions of the mass and stiffness in the model are set such that the modal frequencies are well-separated from each other.

To apply the base excitation, a 120-sec window including 6000 ambient data recorded by one INSN (Iranian National Broadband Seismic Network) station in northern Iran (Charan station, CHTH, ~35.9°N, 51.1°E) is chosen. Data processing (e.g., high-pass filtering, base-line correction) is applied on the raw data to obtain the base excitation history. By performing structural analysis, the absolute acceleration responses are obtained at each DOF.

To simulate the presence of random noise in the real-world cases, the acceleration response data are contaminated by a Gaussian random noise with different levels of intensity. The noise level is defined based on root mean square (rms) similar to that in (Yang *et al*. 2003a). The rms of the signal $z(t)$ is defined as Eq. (13)

$$\mathrm{rms}[z(t)] = \left[\frac{1}{T}\int_0^T z^2(t)dt\right]^{\frac{1}{2}} \tag{13}$$

The contaminating signal is defined by $R_i\, N_i(t)\,\mathrm{rms}[\ddot{z}_i(t)]/\mathrm{rms}[N_i(t)]$, in which $N_i(t)$ is the noise over $\ddot{x}_i^t(t)$ and $R_i$ denotes the level of noise contamination. The three levels of $R_i = 0, 15 \text{ and } 30\%$ is selected for simulating the noisy responses. The required conditions for applying the PP method are fully satisfied in the present example; therefore, the PP method can be employed for the accurate estimation of the center frequencies and bandwidth values in the determination of the modal responses. To apply the PP method, the PSD from the Welch's method using Hamming window with segment length of 64 data and overlap of 25% is constructed. The PSDs obtained from the noisy responses are then averaged and normalized to get the ANPSD from which the modal frequencies can be identified. The ANPSDs of the structure in the frequency range from 0 to 12 Hz with different levels of the noise are depicted in Fig. 1 which shows that the noise contamination has a minor effect on the estimated modal frequencies through the Welch's method. From these spectra, the modal frequencies required for the band-pass filtering process are estimated as 2.1, 5.1 and 8.4 Hz for the first to third modes, respectively.

In order to investigate how the accuracy of the center frequency (i.e., the accuracy of the estimated modal frequency), the selection of the band width value and the noise level affect the results yielded by the proposed method, a parametric study is conducted here. In the study, the center frequency is varied from $0.8f_j$ to $1.2f_j$ and the bandwidth is varied with four values which are 0.25, 0.5, 1 and 2 Hz; the noise levels are the same as those mentioned above. Applying a zero-phase Butterworth band-pass filter of forth order and EMD thereafter, the absolute modal responses at each DOF are obtained. To extract mode shapes, a normalizing DOF should be selected; among the DOFs, the first one is selected for the normalization process (i.e., $q = 1$).

To evaluate correlations between the identified and theoretical mode shapes, the mode assurance criterion (MAC) can be applied. The MAC between two mode shapes of $\mathbf{\Phi}_a$ and $\mathbf{\Phi}_b$ is defined as $\mathrm{MAC}(\mathbf{\Phi}_a, \mathbf{\Phi}_b) = (\mathbf{\Phi}_a^T \mathbf{\Phi}_b)^2 / (\mathbf{\Phi}_a^T \mathbf{\Phi}_a \times \mathbf{\Phi}_b^T \mathbf{\Phi}_b)$ . The MAC values vary between 0 and 1. The 0 and 1 values respectively indicate perfect independence and perfect dependence between two mode shapes. Fig. 2 shows the MAC values between the identified and theoretical mode shapes obtained by varying the different parameters within the specified ranges.

From Figs. 2(a) to 2(d), first, it is observed that the results obtained by the proposed method are not significantly sensitive to the variation of the bandwidth values if an accurate estimate of the modal frequencies (e.g., $0.95f_j$ or $1.05f_j$ ) are used, as it is expected for the systems with well-separated modal frequencies; second, the rather accurate modal frequencies (e.g., $0.90f_j$ or $1.10f_j$ ) are sufficient for the proposed method to yield the valid modal vectors even under high level of the noise contamination (i.e., $R_i = 30\%$); and third, the larger values of the bandwidth result in the formation of a plateau over the modal frequency, which reduces the inaccuracies caused by the relatively poor frequency estimation.

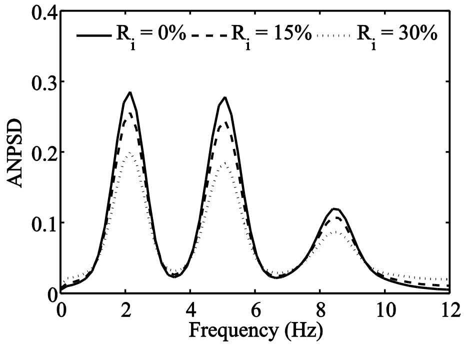


Fig. 1 ANPSDs obtained from simulated responses under different levels of noise

Table 1 Modal parameters of an analytical model

| Mode | Frequency (Hz) | Damping ratio (%) | Mode scale DOF 1 | Mode scale DOF 2 | Mode scale DOF 3 |
|---|---|---|---|---|---|
| 1 | 2.12 | 5.0 | 1.00 | 1.82 | 2.82 |
| 2 | 5.03 | 4.1 | 1.00 | 1.00 | –1.00 |
| 3 | 8.46 | 5.0 | 1.00 | –0.82 | 0.18 |

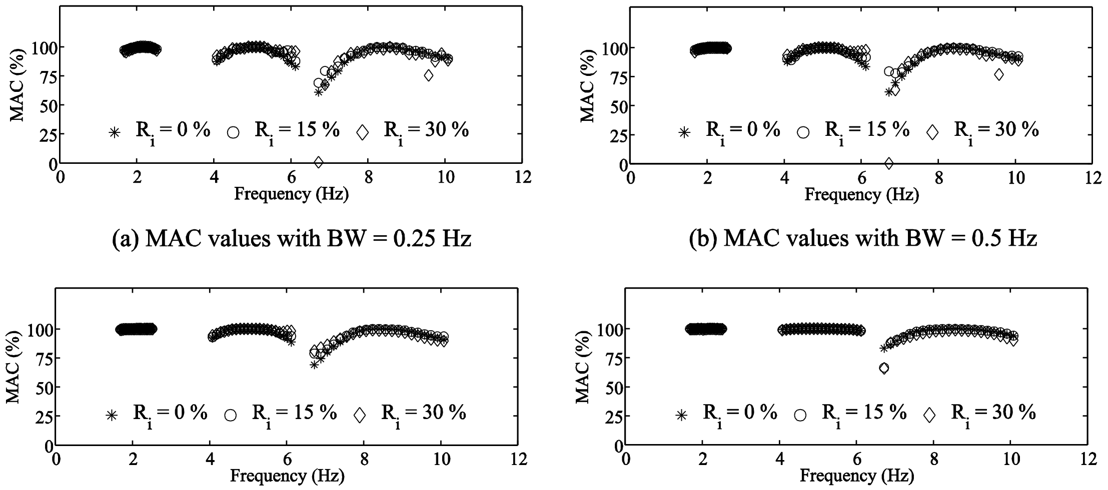


(a) MAC values with BW = 0.25 Hz (b) MAC values with BW = 0.5 Hz

(c) MAC values with BW = 1 Hz (d) MAC values with BW = 2 Hz

Fig. 2 MAC values between identified and theoretical mode shapes obtained from different ranges of center frequency, noise level and bandwidth

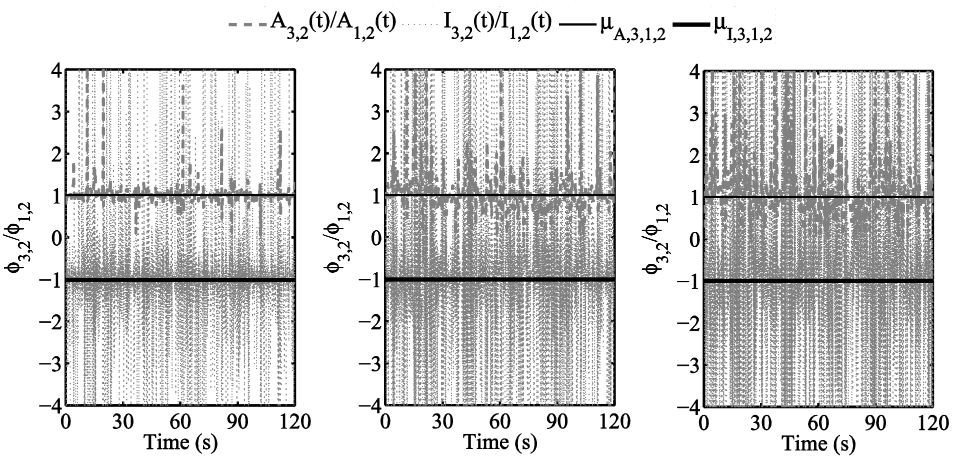


(a) $\phi_{3,2}/\phi_{1,2}$ with $R_i = 0$ % (b) $\phi_{3,2}/\phi_{1,2}$ with $R_i = 15$ % (c) $\phi_{3,2}/\phi_{1,2}$ with $R_i = 30$ %

Fig. 3 Parameters related to calculation of $\phi_{3,2}/\phi_{1,2}$

To show the efficacy of the proposed method in reducing undesired fluctuations in the determination of the ratio of the modal elements, the parameters related to the calculation of $\phi_{3,2}/\phi_{1,2}$ with center frequency of 5.61 Hz (i.e., $1.1f_2$)and bandwidth of 1 Hz under the different levels of noise contamination is shown in Fig. 3. In absence of noise in Fig. 3(a), it can be seen that the use of $A_{3,2}(t)/A_{1,2}(t)$ instead of $I_{3,2}(t)/I_{1,2}(t)$ efficiently reduces physically meaningless fluctuations and provides a very stable trend; the nearly-constant trend in $A_{3,2}(t)/A_{1,2}(t)$ matches the true trend (i.e., the perfect constant ratio) in a LTI system.

In presence of noise in Figs. 3(b) and 3(c), the level of the fluctuations increases in both $A_{3,2}(t)/A_{1,2}(t)$ and $I_{3,2}(t)/I_{1,2}(t)$ as the level of noise increases, yet the former is less affected. Also, it can be observed that $\mu_{A,3,1,2}$ and $\mu_{I,3,1,2}$ yielded from the proposed mean estimator, excellently fit the true constant trends in $A_{3,2}(t)/A_{1,2}(t)$ and $I_{3,2}(t)/I_{1,2}(t)$ respectively almost independent of the level of the noise contamination.

### *4.2 The UCLA factor building*

The Factor Building is a 15-story steel moment-resisting frame structure located in the University of California, Los Angeles (UCLA) shown in Fig. 4. After the 1994 Northridge earthquake, the US Geological Survey instrumented the Factor Building with a sensor network throughout its entire height. The databases collected from the Factor Building present a valuable resource for research in the fields of system identification, structural monitoring and damage detection. Up to now, several studies have been conducted to identify the modal characteristics of the Factor Building (e.g., Skolnik *et al*. 2006, Nayeri *et al*. 2008, Hazra B and Narasimhan 2010).

Skolnik *et al*. (2006), by use of earthquake and ambient vibration data, identified the modal parameters of the building. They employed the stochastic subspace identification method to identify the structural modal frequencies, damping ratios, and mode shapes corresponding to the first nine modes of the building. In their work, the frequencies and mode shapes identified from the low-amplitude earthquake response data are used to update a three-dimensional finite element model of the building which is then used for response prediction of the building. In the modeling, it is assumed that floor diaphragms at all levels are rigid with three in-plane DOFs. The mass and stiffness matrices each of order $45\times 45$ are extracted from the updated model in (Skolnik *et al*. 2006).

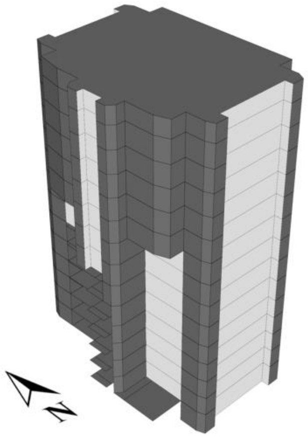


Fig. 4 Layout of the UCLA Factor Building above the ground level

Nayeri *et al*. (2008) by use of ambient vibration records carried out a comprehensive study on the modal characteristics of the building and their uncertainties. The eigen system realization algorithm in conjunction with the natural excitation technique and the chain identification technique as two identification methods, are applied in (Nayeri *et al*. 2008) to extract the modal parameters of the building. Hazra and Narasimhan (2010) employed the second-order blind identification technique and also two other techniques for identification of the modal parameters of the building using both ambient and earthquake responses.

According to (Skolnik *et al*. 2006), recorded data during 2004 Parkfield, California, earthquake are processed to establish a data set including east-west, north-south and torsional floor accelerations. In the data set, the floor acceleration in each direction includes 3400 data points with sampling rate of 20 Hz. Detailed information about data acquisition and data processing can be found in (Skolnik *et al*. 2006). Having the recorded data at all floors in the earthquake data set, the mode shapes of the building can be identified completely. Since the building is weakly excited during the earthquake, the structural behavior can be supposed to be almost linear; hence, linear modal identification can be applied.

Type of the structural system and also regular configurations of the building imply that the PP method is able to properly estimate the modal frequencies of the structure. Similar to previous case, the PSD from the Welch's method using Hamming window with segment length of 64 data and overlap of 25% is applied. To get the estimates of the modal frequencies, the ANPSDs obtained from the acceleration responses of east-west, north-south and torsional directions are obtained as shown in Fig. 5. From the ANPSDs of east-west and north-south directions, three peaks are clearly recognizable below 3 Hz. In the spectrum related to the torsional direction, four peaks are apparent within 0 to 5 Hz.

The identified frequencies by the PP method for east-west and north-south directions are presented in Table 2. The identified values show that the stiffness of the building in north-south direction is slightly higher than that in east-west direction. The modal frequencies determined by performing an eigenvalue analysis on the updated mass and stiffness matrices of the building (Skolnik *et al*. 2006) is also presented in Table 2. It is observed that for the first three modes in east-west and north-south directions, the differences between results obtained from the both methods do not exceed 10%.

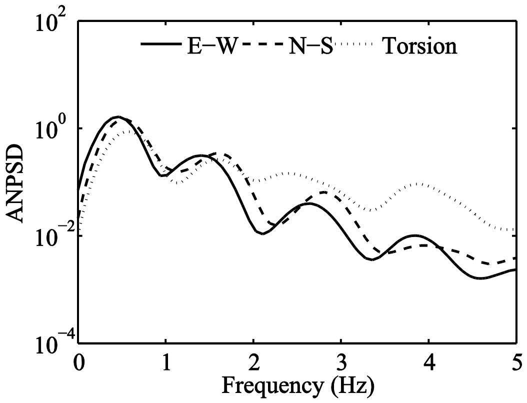


Fig. 5 ANPSDs obtained from earthquake responses of the Factor Building

Table 2 Estimated modal frequencies for the first nine modes of the Factor Building

| Mode | Modal frequencies (Hz) | | | | | | | | |
|---|---|---|---|---|---|---|---|---|---|
| | PP method | | | Updated model (Skolnik *et al*. 2006) | | | Diff (%) | | |
| | E-W | N-S | Tor | E-W | N-S | Tor | E-W | N-S | Tor |
| 1 | 0.5 | 0.5 | 0.6 | 0.473 | 0.514 | 0.691 | 5.7 | –2.7 | –13.2 |
| 2 | 1.4 | 1.6 | 2.4 | 1.507 | 1.670 | 2.319 | –7.1 | –4.2 | 3.5 |
| 3 | 2.7 | 2.8 | 3.9 | 2.580 | 2.761 | 3.743 | 4.7 | 1.4 | 4.2 |

With respect to the height of the building, the location of the fourth floor is distant enough from the location of the nodes in the first three modes of each direction. As a result, the DOFs of the fourth floor are selected as the normalizing DOFs to extract the first three mode shapes in each direction. Applying a zero-phase band-pass filtering with bandwidth of 0.5 Hz and EMD, the complete mode shapes are obtained. The identified mode shapes for east-west and north-south directions together with those extracted from the eigenvalue analysis are depicted in Figs.6and7. All the presented shape vectors are scaled to have unit norms.

For the torsional direction, as noted, the four peaks are apparent in the ANPSD of Fig. 5, which are located at 0.6, 1.6, 2.4 and 3.9 Hz, respectively. Among these peaks, those at 1.6 Hz and 2.4 Hz are relatively close to each other implying that they are related to the same structural mode. Fig.8 shows the extracted mode shapes corresponding to the frequency components of1.6 Hz and 2.4 Hz. It is obvious that the both shapes belong to the second structural mode, but the one corresponding to the 2.4 Hz component slightly better matches the theoretical shape similar to those in Figs. 6(b) and 7(b); as a result, the mode shape corresponding to the frequency component of 1.6 Hz is identified as the second torsional mode shape of the building.

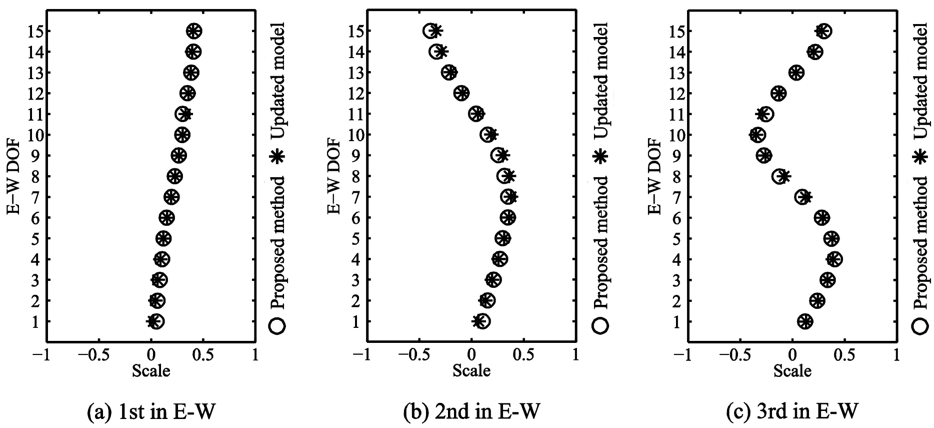


Fig. 6 Identified mode shapes for the Factor Building in east-west direction obtained by the proposed method and the updated model (Skolnik *et al*. 2006)

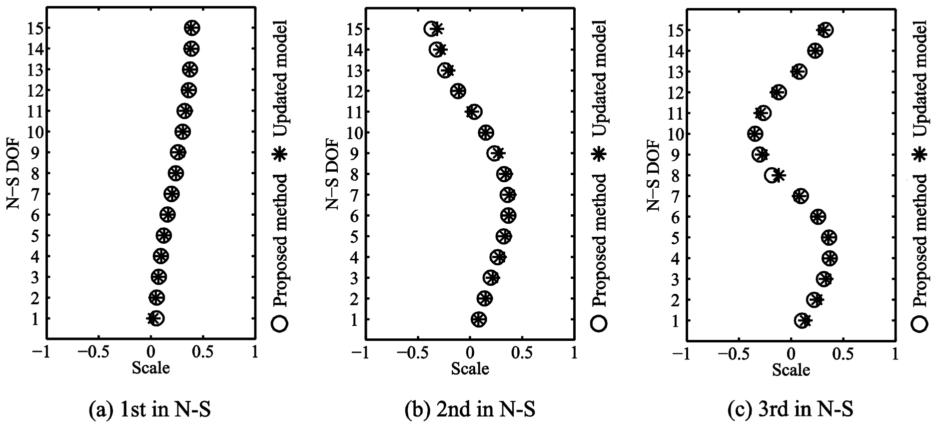

Fig. 7 Identified mode shapes for the Factor Building in north-south direction obtained by the proposed method and the updated model (Skolnik *et al*. 2006)

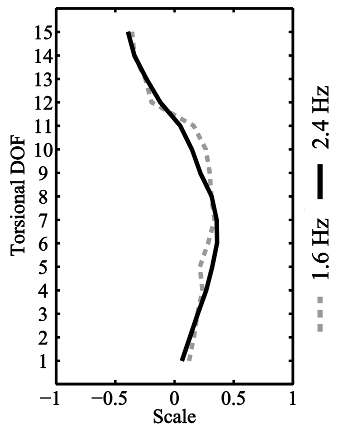

Fig. 8 Identified mode shapes for the Factor Building in torsional direction corresponding to 1.6 Hz and 2.4 Hz components

From a different point of view, if the forms of the mode shapes are well known (either experimentally or computationally), the proposed method can be easily applied for the validation of the estimated modal frequencies. For a regular building structure (i.e., the building which does not contain significant irregularities in structural architecture and also in mass and stiffness proportions) such as the one studied here, the mode shapes in two major translational and torsional axes conform to those theoretically expected for a cantilever column in which the *j*th mode shape in a specified direction contains $j-1$ nodes. This property can be used as a criterion to exclude the frequency components that result in the mode shapes that do not conform to the known forms, as it is done for the torsional frequency component of 1.6 Hz. The identified mode shapes for the torsional direction are presented in Fig.9and their corresponding frequencies are given in Table 2.

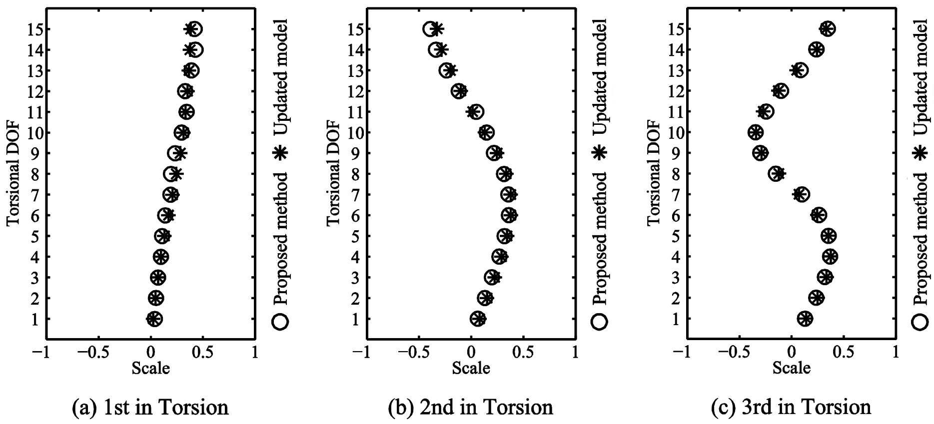


Fig. 9 Identified mode shapes for the Factor Building in torsional direction obtained by the proposed method and the updated model (Skolnik *et al*. 2006)

Table 3 MAC values between identified mode shapes obtained by the proposed method and those correspondingly from the updated model (Skolnik *et al.* 2006)

| Mode | MAC (%) | | |
|---|---|---|---|
| | E-W | N-S | Tor |
| 1 | 99.7 | 99.8 | 98.7 |
| 2 | 98.6 | 99.1 | 98.5 |
| 3 | 99.4 | 99.0 | 99.4 |

The MAC values between the mode shapes obtained by the proposed method and those from the updated model are given in Table 3. It can be seen that the results are in a very good agreement with each other even for the first torsional mode shape which is extracted based on a less accurate estimated center frequency. For the second torsional mode, the MAC value between the mode shape extracted from the frequency component of 1.6 Hz and that from the updated model is 91.1 % which is relatively smaller than the value of 98.5% in Table 3. This difference is directly related to the deviations in the mode shape corresponding to the component of 1.6 Hz (Fig. 8).

With the results from the presented case studies dealt with the simulated and real structural responses, the verification of the proposed method is demonstrated.

## 5. Conclusions

Based on empirical mode decomposition (EMD), as the key part of Hilbert-Huang transform, a simple and efficient method for output-only identification of mode shapes of linear structures subjected to ambient excitations was proposed. To apply the proposed method, measured structural responses are first analyzed by the peak picking method to provide the accurate estimates of the modal frequencies and after that, the estimated modal frequencies are used by the band-pass filter and EMD technique to estimate the modal responses, which are then processed by a proposed robust mean estimator to determine the ratio of the modal elements.

The accuracy and efficacy of the proposed method was investigated in two case studies. In the first case, numerically simulated response data obtained from an analytical 3-story building model with known modal properties are analyzed. From the parametric study carried out in this case, it was found that: first, for a structure with non-closely-spaced modal frequencies, the estimated mode shapes are not significantly sensitive to the variation of the bandwidth applied in the band-pass filter and EMD technique for the isolation of the modal responses, and second, the rather accurate estimates of the modal frequencies are sufficient for the proposed method to provide the valid mode shapes even under high level of noise contamination.

The low-amplitude earthquake response data recorded from the UCLA Factor Building are processed in the second case and the first three mode shapes of the building in east-west, north-south and torsional directions were extracted. In this case, the results from the proposed method are compared with those obtained from the existing updated model of the building. This comparison demonstrated the excellent correlation between the results. Also, it was found that the proposed method can be employed for validation of the estimated modal frequencies if the general forms of the mode shapes are known. Finally, it is concluded that the proposed method with its simplicity and remarkable accuracy offers a very efficient tool for output-only modal identification purposes.

## References

Bahar, O. and Ramezani, S. (2014), "Enhanced Hilbert–Huang transform and its application to modal identification", *Struct. Des. Tall Spec.*, **23**(4), 239-253.

Bao, C., Hao, H., Li, Z.X. and Zhu X. (2009), "Time-varying system identification using a newly improved HHT algorithm", *Comput. Struct.*, **87**(23-24), 1611-1623.

Chopra, A.K. (2001), *Dynamics of Structures: Theory and application to Earthquake Engineering*, Prentice-Hall, Upper Saddle River, New Jersey, USA.

Cunha, A. and Caetano, E. (2006), "From input-output to output-only modal identification of civil engineering structures", *SAMCO Final Report*, University of Porto, Porto, Portugal.

Hazra, B. and Narasimhan, S. (2010), "Wavelet-based blind identification of the UCLA Factor building using ambient and earthquake responses", *Smart Mater. Struct.*, **19**(2), 1-10.

Huang, N.E., Shen, Z., Long, S.R., Wu, M.C., Shih, H.H., Zheng, Q. *et al*. (1998), "The empirical mode decomposition and the Hilbert spectrum for nonlinear and non-stationary time series analysis", *Proceedings of Royal Society of London Series A*, **454**, 903-995.

Huang, N.E. and Bethesda, M.D. (2005), "Computing instantaneous frequency by normalizing Hilbert transform", *US Patent 6901353*.

Liu, B., Riemenschneider, S. and Xu, Y. (2006), "Gearbox fault diagnosis using empirical mode decomposition and Hilbert spectrum", *Mech. Syst. Signal Pr.*, **20**, 718-734.

Liu, TY., Chiang, W.L., Chen, C.W., Hsu, W.K., Lin, C.W., Chiou, D.J. and Huang, P.C. (2012), "Structural system identification for vibration bridges using the Hilbert–Huang transform", *J. Vib. Control*, **18**(13), 1939-1956.

Nayeri, R.D., Masri, S.F., Ghanem, R. and Nigbor, R.L. (2008), "A novel approach for the structural identification and monitoring of a full-scale 17-story building based on ambient vibration measurements",

*Smart Mater. Struct.*, **17**(2), 1-19.
Poon, C.W. and Chang, C.C. (2007), "Identification of nonlinear elastic structures using empirical mode decomposition and nonlinear normal modes", *Smart Struct. Syst.*, **3**(4), 423-437.
Rilling, G., Flandrin, P. and Goncalves, P. (2003), "On empirical mode decomposition and its algorithms", *Proceedings of the IEEE-EURASIP Workshop on Nonlinear Signal and Image Processing*, Grado, Italy.
Skolnik, D., Lei, Y., Yu, E. and Wallace, J.W. (2006), "Identification, model updating, and response prediction of an instrumented 15-story steel-frame building", *Earthq. Spectra*, **22**(3), 781-802.
Wang, Z. and Chen, G. (2012), "Recursive Hilbert-Huang Transform method for time-varying property identification of linear shear-type buildings under base excitations", *J. Eng. Mech. - ASCE*, **138**(6), 631-639.
Wu, Z. and Huang, N.E. (2008), "Ensemble Empirical Mode Decomposition: a noise-assisted data analysis method", *Adv. Adapt. Data Anal.*, **1**(1), 1-41.
Xu, Y.L., Chen, S.W. and Zhang R.C. (2003), "Modal identification of Di Wang Building under Typhoon York using the Hilbert–Huangtransform method", *Struct. Des. Tall Spec.*, **12**(1), 21-47.
Yan, B. and Miyamoto, A. (2006), "A comparative study of modal parameter identification based on wavelet and Hilbert–Huang transforms", *Comput. -Aided Civil Infrastruct. E.*, **21**(1), 9-23.
Yang, J.N. and Lei, Y. (2000), "System identification of linear structures using Hilbert transform and empirical mode decomposition", *Proceedings of the 18th International Modal Analysis Conference: A Conference on Structural Dynamics*, San Antonio, TX, Society for Experimental Mechanics Inc., Bethel, CT.
Yang, J.N., Lei, Y., Pan, S. and Huang, N.E. (2003a), "System identification of linear structures based on Hilbert-Huang spectral analysis Part 1: Normal modes", *Earthq. Eng. Struct. D.*, **32**(9), 1443-1467.
Yang, J.N., Lei, Y., Pan, S. and Huang, N.E. (2003b), "System identification of linear structures based on Hilbert-Huang spectral analysis Part 2: Complex modes", *Earthq. Eng. Struct. D.*, **32**(10), 1533-1554.
Yang, J.N., Lei, Y., Lin, S. and Huang, N.E. (2004), "Identification of natural frequencies and dampings of in situ tall buildings using ambient wind vibration data", *J. Eng. Mech. - ASCE*, **130**(5), 570-577.
Zhang, R.C., Ma, S., Safak, E. and Hartzell, S. (2003), "Hilbert–Huang transform analysis of dynamic and earthquake motion recordings", *J. Eng. Mech. - ASCE*, **129**(8), 861-875.

*CC*